RESEARCH ARTICLE

Editorial Process: Submission:12/13/2022 Acceptance:04/07/2023

Aberrant Expression of FGFRL1 in Esophageal Cancer and Its Regulation by miR-107

Priyanka Sharma[1,2], Vaishali Kaushik[1], Anoop Saraya[3], Rinu Sharma[1]*

Abstract

Background: Fibroblast growth factor receptors are growth factor receptor tyrosine kinases, exerting their roles in embryogenesis, tissue homeostasis, and development of cancer. However, little is known about the expression and function of FGFRL1 in esophageal cancer (EC). **Methods:** We systematically evaluated the expression of FGFRL1 in TCGA and GETex datasets followed by expression analysis in EC cell lines and clinical specimens using immunofluorescence (IF) and immunohistochemistry (IHC) respectively. **Results:** GEPIA analysis on TCGA and GETex datasets identified significant upregulation of FGFRL1 in EC patients (n=182) compared to normal controls (n=286, $p<0.05$). IHC analysis showed significantly higher FGFRL1 expression in EC tissues as compared to the distant matched non-malignant tissues ($p<0.001$). Immunoflourescence in EC cells suggested increased expression of FGFRL1 from WDSCC (KYSE30) to MDSCC (KYSE140) and finally to PDSCC (KYSE410). In-silico tools predicted miR-107 as most significant miRNA regulating FGFRL1 expression. qRT-PCR revealed miR-107 expression to be significantly and inversely correlated with FGFRL1 expression in 73% (22/30) EC tissues ($p=0.015$) and over-expression of miR-107 resulted in significantly decreased expression of FGFRL1 at mRNA (fold change=0.11, $p=0.0016$) as well as protein level in miR-107 versus NC treated cells. Luciferase reporter assay using FGFRL1-3'UTR further confirmed it to be a direct target of miR-107. **Conclusion:** Our results herein document clinical as well as functional relevance of FGFRL1 in EC and its regulation by miR-107.

Keywords: Esophageal squamous cell carcinoma- Fibroblast growth factor receptor- miRNA mediated regulation- TCGA

Asian Pac J Cancer Prev, **24 (4)**, 1331-1341

Introduction

Fibroblast growth factor receptors (FGFRs) are high affinity cell surface tyrosine kinase receptors, exerting their roles in embryogenesis, tissue homeostasis, and implicated in development of cancer. Mutations and aberrant expression of FGFR 1-4 promote the initiation and progression of bladder and prostate cancer (Turner and Grose, 2010). Aberrant activation of FGFRs promote tumorigenesis by increasing cell proliferation, migration, survival and differentiation. Fibroblast growth factor receptor like 1 (FGFRL1) is the poorly understood member of FGFR family and shows up to 40% amino acid sequence similarity to other FGFRs (Wiedemann et al., 2000; Rieckmann et al., 2009) but lack kinase domain (Olsen et al., 2007; Wesche et al., 2011; Yang et al., 2017; Bonifacino et al., 2003; di Martino et al., 2013). The FGFRL1 gene is expressed in all vertebrates albeit at lower levels than that of conventional FGFRs. In human, FGFRL1 mRNA is expressed at a high level in pancreas, thyroid and adrenal gland, kidney, skeletal muscle and heart. Whereas, the expression is negative in lung, stomach, esophagus, and smooth muscle (di Martino et al., 2013; Tsuchiya et al., 2011). In contrast to other FGFRs, FGFRL1 has been shown to act as a decoy receptor to FGF ligands and antagonizes FGFR signalling in early development (Steinberg et al., 2010) and inhibits cell proliferation. Antagonistic effect of FGFRL1 on FGFR signalling as a decoy receptor has been reinforced by its lack of kinase domain and interaction with Spred1, a negative regulator of FGF (Trueb et al., 2003; Steinberg et al., 2010; Zhuang et al., 2011). However, this negative regulation theory has been challenged by the presence of genes that are regulated by FGFRL1. Emerging evidences suggest that cytoplasmic domain of FGFRL1 contains an SH2 binding motif that interacts with the tyrosine phosphatase SHP1 and overexpression of Fgfrl1 results in activation of ERK1/2 signaling (Silva et al., 2013). Chen et al., (2020) also demonstrated FGFRL1 mediated regulation of ENO1-PI3K/Akt pathway via combining to ENO1 in SCLC cells (Chen et al., 2020). These observations highlighted the oncogenic role of FGFRL1 independent of FGFR signalling.

MicroRNAs play a crucial role in regulating the

*[1]University School of Biotechnology, Guru Gobind Singh Indraprastha University, Dwarka, New Delhi, India. [2]Department of Leukemia, University of Texas MD Anderson Cancer Center, Houston, Texas, USA. [3]Department of Gastroenterology, All India Institute of Medical Sciences, Ansari Nagar, New Delhi, India. *For Correspondence: rinusharma@gmail.com*

expression of various genes and modulate tumor cellular processes. FGF pathway activity during development or regeneration can be regulated by miRNAs and loss of miRNA regulation of FGF signaling can result in disease progression or cancer. Several miRNAs including miR-338, miR-17, miR-424 and miR-503, miR-710, miR-34a have been shown to affect cell differentiation by directly regulating FGF or FGFR expression (Liu et al., 2014; Carraro et al., 2009; Kim et al.,2013 ; Uchiyama et al., 2010; Fu et al., 2014; Liu et al., 2014; Cheng et al., 2014)Decreased expression of FGF/FGFR regulating miRNAs in cancers has been reported thereby leading to upregulation of FGFR mediated signalling and cancer progression (Cheng et al., 2014; Yang et al., 2014 ; Yin et al., 2013). However, limited information is available for miRNA mediated regulation of FGFRL1. miR-210 has been shown to directly regulate FGFRL1 in Esophageal squamous cell carcinoma (ESCC). FGFRL1 promotes proliferation of ESCC cell by inhibiting the cell cycle arrest at the G1/G0 and G2/M phase (Tsuchiya et al., 2011). Later, similar results were observed in osteosarcoma (Liu et al., 2018) bladder cancer (Yang et al., 2017) and hepatocellular carcinoma (Yang et al., 2016) as well. In present study, we have demonstrated the clinical significance of FGFRL1 in EC and identified miR-107 as regulator of FGFRL1 expression.

Materials and Methods

Data mining from TCGA and GTEx datasets

The online database Gene Expression Profiling Interactive Analysis (GEPIA) (http://gepia.cancer-pku.cn/index.html) was used to analyse the expression of FGFRL1 in different cancers including EC as compared to the normal controls. GEPIA is an interactive web that includes 9,736 tumors and 8,587 normal samples from TCGA and the GTEx projects, which analyse the RNA sequencing expression (Silva et al., 2013). GEPIA was used to generate box plots, based on gene expression using Anova on log2 (TPM+1) and |Log2FC| cut-off of 1 in 33 different types of cancers. Differential expression of FGFRL1 in EC was determined on ESCA (TCGA n=182) v/s 286 normal controls (GTEx n=273 + TCGA n=13). $p<0.05$ was considered as statistically significant.

Patients and clinicopathological data collection

This study was approved by the institutional human ethics committee prior to its commencement. Tumor and matched distant non-malignant esophageal tissue biopsy specimens (obtained from a region atleast 8 cm away from the tumor) were collected from patients who underwent endoscopy in Department of Gastroenterology, All India Institute of Medical Sciences, New Delhi, India with the prior consent of patients. The diagnosis was based on clinical examination and histopathological analysis of the tissue specimens. The tumors were histopathologically graded as preneoplastic (30) and neoplastic (21). Seven endoscopic biopsies collected from a region atleast 8 cm away from the tumor were histopathologically confirmed to be non-malignant esophageal tissue. The samples were collected and immediately snap frozen in liquid nitrogen and stored at −80◦C till further use. One part of the sample was collected in 10% formalin and embedded in paraffin was used for hematoxylin/eosin staining and immunohistochemical analysis. The clinicopathological data were recorded in a predesigned performa that included site of lesion, histopathological differentiation, age, gender, nature of diet, tea, alcohol and tobacco consumption, and family history.

Immunohistochemistry

Paraffin-embedded sections (5 μm) of histologically confirmed human esophageal normal (n = 7), preneoplastic tissues (n=30) and ESCC (n = 21) tissues were obtained on poly-L-lysine coated slides. Briefly, the tissue sections were deparaffinized and rehydrated. Tris–EDTA buffer (10 mM Tris-base, 1 mM EDTA, pH 9.0) was used for carrying out antigen retrieval followed by incubation with 0.3% v/v hydrogen peroxide in methanol for 30 min and blocking in 1% normal horse serum. Slides were incubated overnight with rabbit polyclonal anti-FGFRL1 antibody (CloudClone) at 4 °C followed by 30 min incubation with HRP conjugated anti-rabbit IgG (ImmPRESS anti-rabbit Ig (peroxidase) Polymer Detection kit, Vector Laboratories Inc, USA) at RT. The colour was developed using diaminobenzidine as the chromogen. Haematoxylin was used for nuclear staining. Esophageal tissue sections not treated with anti-FGFRL1 antibody were used as negative controls (NC). For FGFRL1 protein expression, sections were counted as positive if epithelial cells showed immunopositivity in the membrane/nucleus/cytoplasm when observed independently by three of us (VK, RS and PD). The slides were scored based on the percentage of immunostained cells as ≤ 10% = 0; 11–20% = 1; 21–40%=2;41–60%=3;61–80%=4and>81%=5. Slides were also scored on the basis of staining intensity as faint = 1; moderate = 2 and strong = 3. Finally, a total score was found by adding the scores of percentage positivity and intensity. Based on sensitivity and specificity, calculated by ROC curve analysis, a total score cut-off value of 4 was defined as FGFRL1 immunopositivity.

Cell culture

Human ESCC cell line KYSE-410 was purchased from the European Collection of Authenticated Cell Cultures (ECACC), supplied by Sigma- Aldrich (Bangalore, India). KYSE-30 and -140 were a kind gift from Dr. Y.Shimada (Japan). The cell culture was maintained in RPMI-1640 medium (Sigma-Aldrich) supplemented with 10% FBS (HiMedia Laboratories Pvt. Ltd., Mumbai, India), 100 U/ml of penicillin and 100 μg/ml of streptomycin (HiMedia Laboratories). The HEK-293T cell line was a kind gift by Dr Nimisha Sharma (GGSIPU, New Delhi). It was maintained in DMEM (HiMedia Laboratories) supplemented with 10% FBS, 100 U/ml of penicillin and 100 μg/ml of streptomycin. The cell lines were maintained in a humidified incubator with 5% CO_2 and 95% humidity at 37℃.

Immunofluorescence microscopy

To determine the localization of FGFRL1 protein in EC cells, confocal and immunofluorescence microscopy

were performed. Briefly, the cells were fixed in methanol at –20 °C for 20 min and permeabilized with 0.5% Triton X-100 in 1X-PBS for 10 min. To prevent non-specific binding, the cells were blocked with 3% BSA and 0.05% Triton X-100 in PBS for 1 h. Then the cells were incubated with rabbit polyclonal anti-FGFRL1 antibody (1:50 dilution) overnight at 4 °C, followed by incubation with Alexa Fluor 488-conjugated goat anti- rabbit secondary antibody (Invitrogen) at room temperature for 30 min (1:1000 dilution). The cells were observed under an inverted fluorescence microscope (Nikon), after nuclei counterstaining with propidium iodide (PI) for immunofluorescence microscopy.

In-silico tools to predict miRNAs regulating FGFRL1

Three miRNA prediction tools viz. miRanda, miRdb and miRNet was used for prediction of potential miRNAs targeting FGFRL1. In order to minimize false positives, only miRNAs predicted by all the three software were selected. The most putative miRNA was further screened out on the basis of number of target sites, type of sites (canonical 8-mers were preferred over canonical 7-mer which were preferred than marginal 6-mers) and their miSVR score as calculated using miRanda.

Transient transfection of miR-107 mimic using Lipofectamine 3000

KYSE-410 cells were seeded in 96-well plates ($1.2x10^4$ cells/well), 24-well plate ($5x10^4$ cells/well) or 6-well plate ($3x10^5$ cells/well). hsa-miR-107 mimic (100 nM) (Ambion, Inc., Foster City, CA, USA) was transfected in the cells using Lipofectamine 3000 (Invitrogen, Carlsbad, CA, USA) and Opti-MEM medium (Invitrogen) according to the manufacturer's instructions. Negative control #1 (Ambion) was used as NC.

RNA extraction and quantitative RT-PCR

Total RNA was extracted using RNeasy Mini Kit (Qiagen) followed by first-strand cDNA synthesis using universal cDNA synthesis kit (Exiqon A/S, Vedbaek, Denmark) according to the manufacturer's protocol. qRT-PCR analysis of miR-107 was performed using SYBR-Green Master Mix (Exiqon A/S) and predesigned miR-107 specific LNATM PCR primer sets (Exiqon A/S) as described previously (Song et al., 2017).

The first strand cDNA for FGFRL1 was synthesized using oligo dT (Fermentas, Canada) and MMLV reverse transcriptase (Fermentas, Burlington, ON, Canada). qRT-PCR of FGFRL1 was carried out using gene-specific primers (Table 1) and KAPA SYBR FAST real-time PCR kit (Kapa Biosystems, Inc., Wilmington, MA, USA) following the manufacturer's protocol. Its expression was analyzed at 48 and 72 h post miR-107 transfection using qRT-PCR. The expression of FGFRL1 mRNA in the mimic-treated cells was normalized to that of the cells treated with NC.

A small RNA, 5S rRNA (Table 1) was used as the endogenous control for data normalization. The $2^{-\Delta\Delta CT}$ method was used to calculate the fold-change.

Western blot analysis

Protein was isolated using RIPA buffer (Invitrogen) supplemented with a protease inhibitor cocktail (Invitrogen) using sonication. 70 µg of protein were separated by 12.5% SDS-PAGE and transferred to PVDF membranes (Microdevices, Inc., New Delhi, India). The membranes were blocked with 5% non-fat milk in PBS overnight at 4 ℃ followed by incubation for 1 h with primary antibodies of FGFRL1 (CloudClone) and GAPDH (Santa Cruz Biotechnology, CA, USA) at dilution of 1:200. The membranes were washed and incubated with the horseradish peroxidase (HRP)-conjugated anti-rabbit secondary antibody (DAKO A/S Copenhagen, Denmark) for 1 h. After washing, bound secondary antibody was detected using enhanced chemi-luminescence (ECL) system (Pierce Biotechnology Rockford, IL, USA). Western blot results were analyzed quantitatively using ImageJ.

FGFRL1 3'UTR reporter construct

FGFRL1 has ten miR-107 MRE (miRNA recognition elements) in 3'UTR of FGFRL1 (MFE of -28.2 Kcal/mol). A 989 bp region of FGFRL1-3'UTR (NM_001004358.1) containing all the ten predicted binding sites for miR-107 was amplified and cloned in pMIR-REPORT luciferase vector (Promega) between the *Mlu*1 and *Hind*III restriction sites, downstream to the luciferase reporter gene using primers as described in Table 1.

Luciferase reporter assay

HEK-293T cells were seeded into 24-well plates and cultured until 80% confluent. The cells were then co-transfected with either miR-107 mimic or NC at a 100 nM final concentration and with 100 ng of pMIR-REPORT construct containing FGFRL1 3'UTR along with 10 ng *Renilla* luciferase vector using Lipofectamine 3000 transfection reagent according to the manufacturer's recommendations (Invitrogen). Relative firefly luciferase activity, which was normalized with *Renilla* luciferase, was measured using a Dual-luciferase reporter gene assay system (Promega) and the results were plotted as the percentage of change over the respective control.

Statistical analysis

All experiments were repeated at least three times and the Student's t-test was used to analyze the statistical significance between two groups while one-way ANOVA was used to determine the significance of differences among multiple groups. $P<0.05$ was considered to indicate a statistically significant difference. Statistical analysis were performed using GraphPad Prism software version 6.00 (GraphPad Software, Inc., CA, USA) and SPSS software 16.0 (SPSS, Inc., Chicago, IL, USA). To assess the diagnostic accuracy, receiver-operating characteristic (ROC) curves were generated and area under the ROC curve (AUC) was determined. The correlation of miR-107 and target gene, FGFRL1 was analyzed using non-parametric Spearman's rho test.

Results

Data mining from TCGA and GTEx datasets

In-silico analysis of FGFRL1 expression in TCGA and GTEx datasets using GOPIA revealed a signficantly decreased expression of FGFRL1 mRNA in 182 EC patients as compared to 286 normal controls ($p<0.05$, Figure 1A and 1B). cBioportal showed alterations in FGFRL1 gene in 11 patients (mutation = 5, amplification = 3, Deletion=3) out of 185 patients in TCGA dataset and in 1 patient out of 88 in ICGC dataset (Figure 1C). 9 patients out of these 12 patients had disease free survival data and alteration in FGFRL1 was significantly associated with poor DFS with median DFS of 8.7 months for patients with alteration as compared to the unaltered group (median =21.4 months) (Figure 1D). Though, it had no significant association with overall survival (p=0.141) (Data not shown).

Increased expression of FGFRL1 protein in ESCC tissues

To determine the clinical significance of FGFRL1 protein in ESCC, its expression and localization was investigated in 21 ESCC tissues, 30 preneoplastic tissues and 7 histologically confirmed distant matched non-malignant esophageal tissues using immunohistochemistry. Increased expression of FGFRL1 protein was observed in 20/21 (95%) ESCC tissues and 13/30 (43%) preneoplastic tissue. FGFRL1 expression was observed in the cytoplasm of EC tissues. A high percentage positivity and increased intensity of FGFRL1

Table 1. Primer Sequences Used in This Study

Primers for qRT-PCR	
FGFRL1 Forward Primer	5' ACACAGCCCTCCAAGATGAG 3'
FGFRL1 Reverse Primer	5' GCAGGTTCTTCAGGCTCAGT 3'
5S rRNA Forward Primer	Forward: 5'- GTCTACGGCCATACCACCCTG-3'
5S rRNA Reverse Primer	Reverse: 5'-AAAGCCTACAGCACCCGGTAT-3'
Primers for cloning	
FGFRL1-ECOR1-Forward Primer	5' GCCGAATTCGTTATGGCCATGACGCCGAGCCCCCTGTT 3'
FGFRL1- Xho1-Reverse Primer	5' CGCCTCGAGCTAGCACTGATAGTGGATGTGCTGGTGGA 3'

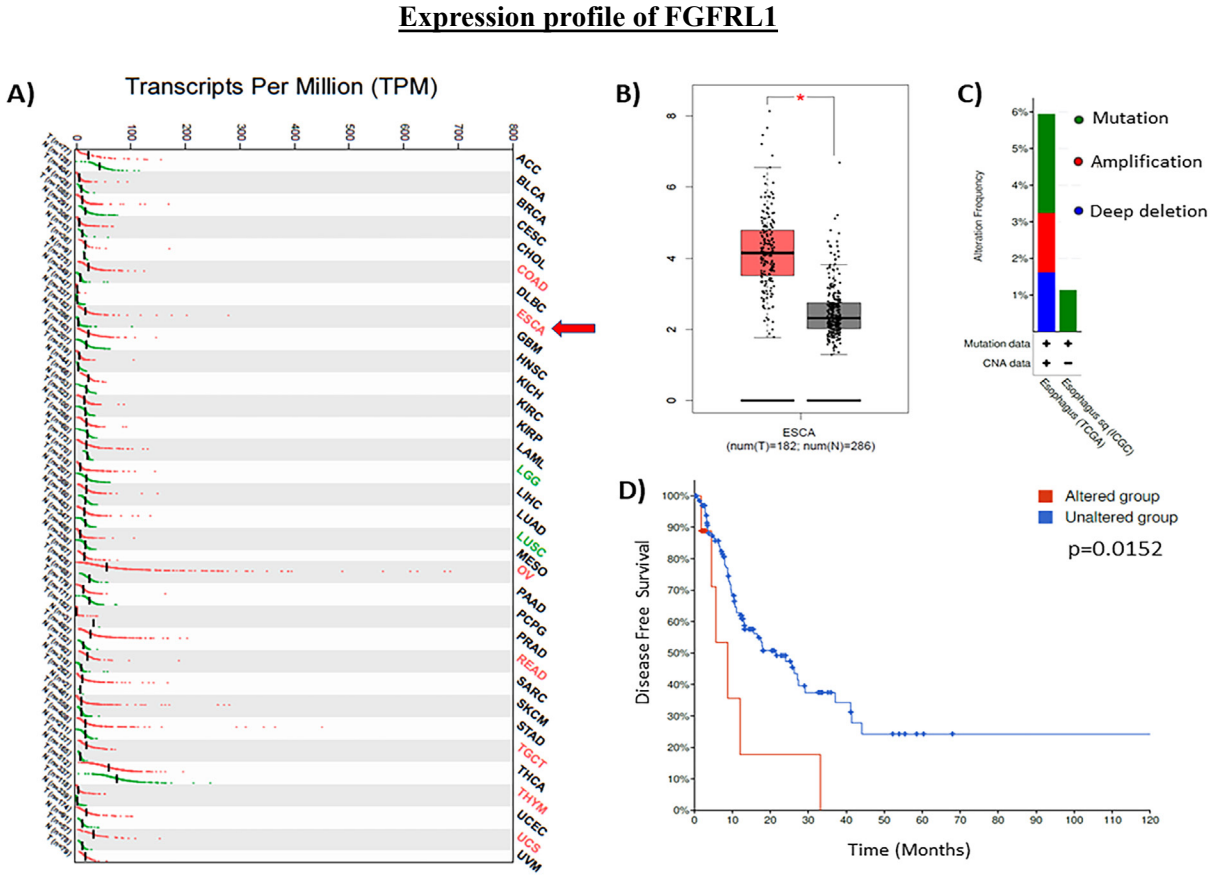

Figure 1. Panel A) Expression profile of FGFRL1 in 33 different cancers including EC from TCGA dataset v/s normal controls obtained from GTEx database. Analysis was performed using GoPIA tool. B) Box plot showing expression of FGFRL1 in EC versus normal controls. C) Diagram showing association of FGFRL1 expression with mutation status in EC patients from TCGA and ICGC datasets. D) Altered FGFRL1 expression was significantly associated with poor disease-free survival.

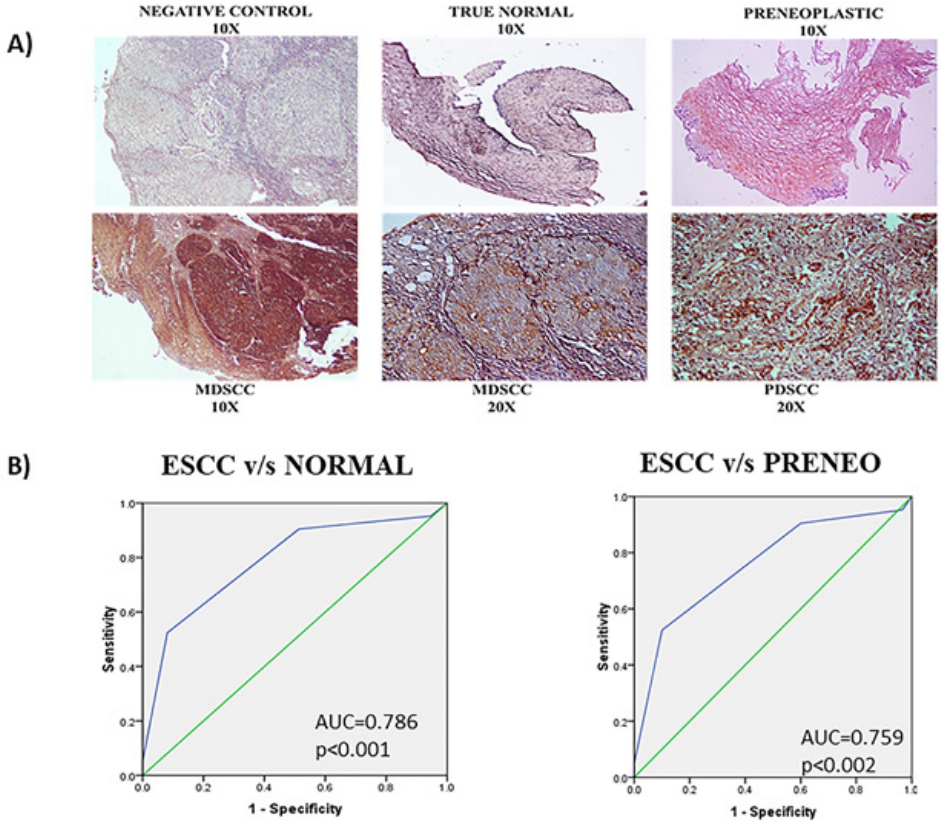

Figure 2. A) Representative esophageal tissue section immunostained for FGFRL1 in (a) NC showing no detectable FGFRL1 (no primary antibody) (b) histologically normal tissue showing no immunoreactivity (c) preneoplastic tissue showing cytoplasmic immunoreactivity (d&e) moderately differentiated tissue showing intense cytoplasmic and membranal staining (f) poorly differentiated section showing even darker staining. B) ROC analysis for FGFRL1 protein expression in ESCC tissues as compared to preneoplastic tissues and normal controls.

staining was observed in ESCC tissues as compared to distant matched non-malignant tissues which either did not show any detectable staining for FGFRL1 protein or a very faint staining in lesser proportion of cells in the tissues was observed (Figure 2A). Student t-test showed a significant increase in FGFRL1 protein expression in ESCC tissues as compared to distant non-malignant tissues ($p<0.001$, Table 2).

ROC analysis revealed an AUC of 0.786 with sensitivity of 90.47% and specificity of 48.64% (Figure 2B). However, no significant correlation was observed between FGFRL1 protein expression in tissues and clinicopathological parameters (Table 2).

FGFRL1 protein localizes in the cytoplasm and the membrane of ESCC cells

Expression and localisation of FGFRL1 was analysed in EC cell lines (KYSE30, KYSE140 and KYSE410) varying

Table 2. Relationship of FGFRL1 Protein Expression with Clinicopathological Parameters of ESCC Patients

Clinicopathological Parameters	Total Cases	FGFRL1 protein positivity n (%)	p-value
Distant matched non-malignant	7	1 (14)	
ESCC	21	20 (95)	<0.001
Age (years)			
<40	10	7 (70)	>0.05
≥40	49	23 (92)	
Gender			
Male	30	19 (30)	>0.05
Female	29	11 (29)	
Histopathology grading			
MDSCC/PDSCC	21	19 (21)	>0.05
PRENEO	30	18 (30)	

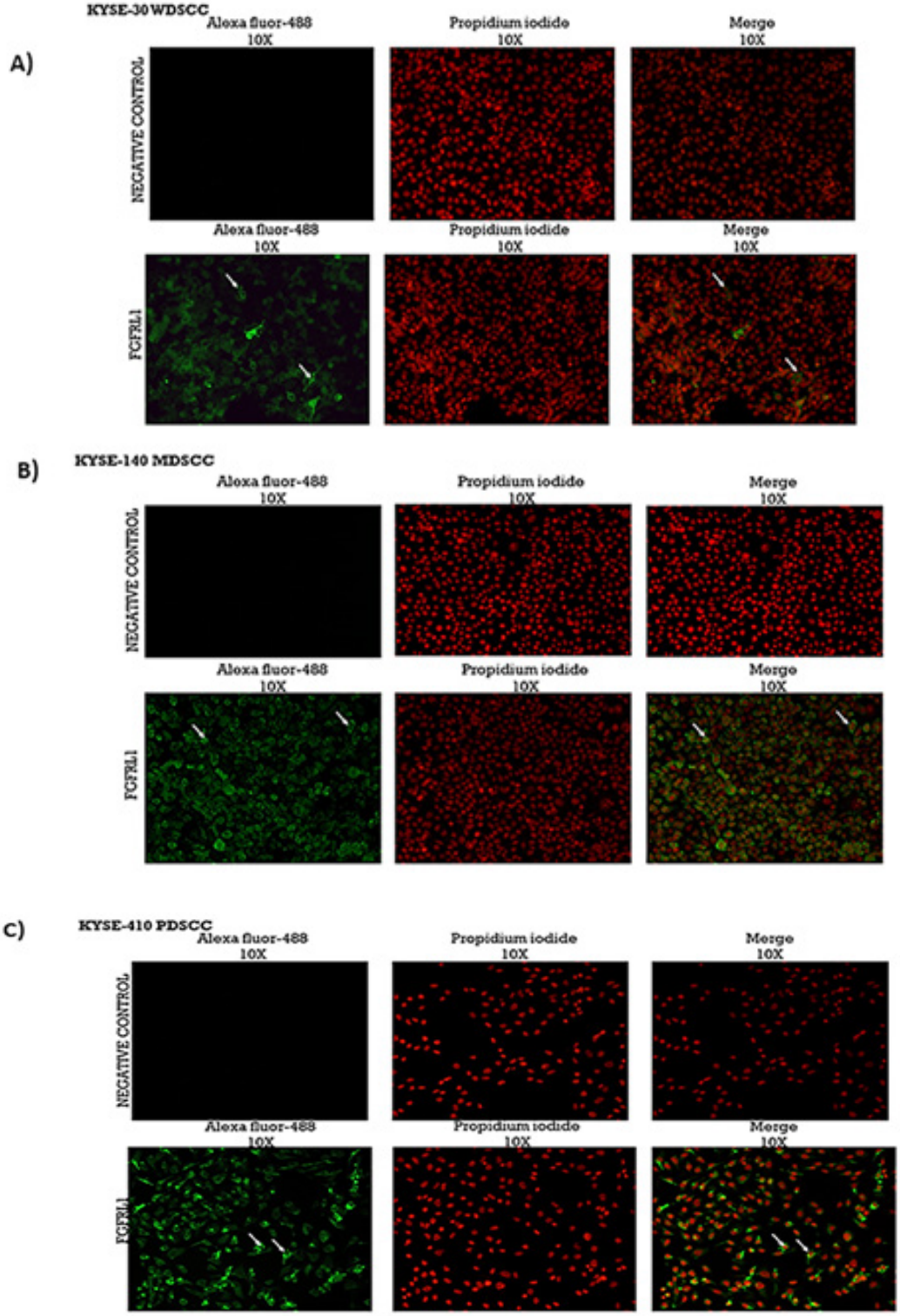

Figure 3. A) Subcellular distribution of FGFRL1 in WDSCC (KYSE30): The top panel shows fluorescence emitted from the antibody (green; absent), cell nuclei (red) stained with PI and the nuclear presence of the antibody (yellow; absent) as demonstrated by superimposition of the two images. Similarly, the lower panel show the fluorescence emitted from the antibody(green), cell nuclei (red) stained with PI and the nuclear presence of the antibody (yellow; absent) as demonstrated by superimposition of the two images (Magnification: 10X). B) Subcellular distribution of FGFRL1 in MDSCC cells (KYSE140): The top panel shows fluorescence emitted from the antibody (green; absent), cell nuclei (red) stained with PI and the nuclear presence of the antibody (yellow; absent) as demonstrated by superimposition of the two images. Similarly, the lower panel show the fluorescence emitted from the antibody(green), cell nuclei (red) stained with PI and the nuclear presence of the antibody (yellow; absent) as demonstrated by superimposition of the two images (Magnification: 10X). C) Subcellular distribution of FGFRL1 in PDSCC cells (KYSE410): The top panel shows fluorescence emitted from the antibody (green; absent), cell nuclei (red) stained with PI and the nuclear presence of the antibody (yellow; absent) as demonstrated by superimposition of the two images. Similarly, the lower panel show the fluorescence emitted from the antibody(green), cell nuclei (red) stained with PI and the nuclear presence of the antibody (yellow; absent) as demonstrated by superimposition of the two images (Magnification: 10X).

Table 3. List of miRNAs Predicted by *insilico* Analysis as Potential Regulators of FGFRL1 Expression

miRanda	miRDB (71)	miRNet
miR-103 miR-107 miR-371-5p miR-210 miR-495 miR-150 miR-34c-5p miR-34a miR-449a miR-449-b	miR-889-3p, miR-7-2-3p, miR-7157-5p, miR-7157-3p, miR-7-1-3p, miR-7111-5p, miR-103a-3p, miR-107, miR-6891-3p, miR-6889-3p, miR-6870-5p, miR-6818-5p, miR-6798-5p, miR-6787-5p, miR-6754-5p, miR-6749-3p, miR-6737-3p, miR-6736-3p, miR-663a, miR-661, miR-656-3p, miR-6529-3p, miR-6504-3p, miR-618, miR-6072, miR-593-3p, miR-5698, miR-5688, miR-567, miR-520b-5p, miR-519a-2-5p, miR-5008-3p, miR-495-3p, miR-4800-3p, miR-4793-3p, miR-4723-5p, miR-4692, miR-4686, miR-4666b, miR-4520-5p, miR-4514, miR-4455, miR-4442, miR-4441, miR-4310, miR-4288, miR-4270, miR-3922-3p, miR-371a-5p, miR-3190-5p, miR-3175, miR-3158-5p, miR-3130-3p, miR-302c-5p, miR-302a-5p, miR-2114-5p, miR-210-3p, miR-198, miR-1973, miR-1908-5p, miR-1227-5p, miR-10524-5p, miR-10401-3p, miR-10399-5p, miR-10396b-5p, miR-10226, miR-3657, miR-4673, miR-4669, miR-6867-5p, miR-4645-5p	miR-3130-3p, miR-21-5p, miR-6867-5p, miR-4658, miR-7157-5p, miR-335-5p, miR-107, let-7b-5p, miR-574-5p, miR-6765-5p, miR-103a-3p, miR-3659, miR-1304-5p, miR-1827, miR-6790-5p, miR-6818-5p, miR-140-5p, miR-210-3p, miR-4793-3p

in histopathological grades using immunofluorescence assay. Specific staining was observed in cytoplasm and membrane as a positive staining (green) for FGFRL1 protein expression. Nucleus was stained (red) using PI. Upon merging the two images no nuclear localisation (yellow) was observed i.e. the expression is negative for nucleus. NC (lacking primary antibody) showed no signal from the antibody (i.e. no FGFRL1 expression). Also, the expression seemed to be increasing as we progressed from WDSCC (KYSE 30) to MDSCC (KYSE 140) and finally to PDSCC (KYSE 410) (Figure 3A-C).

In-silico prediction of miRNAs regulating FGFRL1

Putative miRNAs targeting FGFRL1 were predicted using miRanda, miRdb and miRNet as shown in Figure 4A and Table 3. miRdb identified 71 miRNAs while miRanda and miRNet resulted in 10 and 20 potential miRNAs respectively. Three miRNAs viz. miR-107, miR-103 and miR-210 were identified by all the three tools. Notably, FGFRL1 is a validated and well-established target

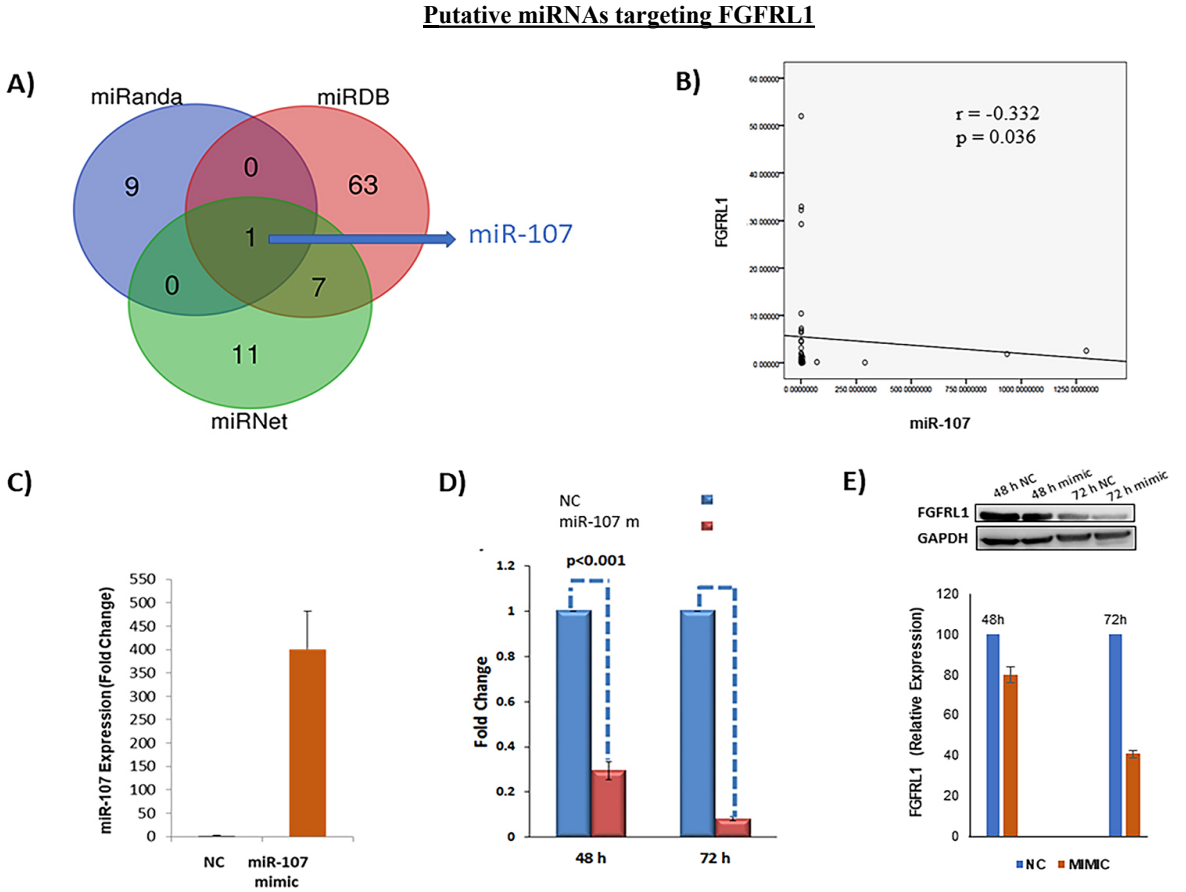

Figure 4. A) Insilico analysis for predicting putative miRNAs targeting FGFRL1: Prediction of miRNAs regulating FGFRL1 using different tools (Miranda, miRDB, mirnet). B) Non-parametric Spearman's rho test showing negative correlation between miR-107 and FGFRL1 in clinical cohort of EC patients identified by qRT-PCR C) Histogram showing fold-change in miR-107 expression at 72 h post-transfection in KYSE-410 cells. D) Overexpression of miR-107 resulted in significantly decreased expression of FGFRL1 mRNA at 48h and 72 h post transfection. E) Effect of miR-107 overexpression on FGFRL1 protein levels in the KYSE-410 cells. The relative expression of Cdc42 protein was calculated as band intensity of FGFRL1/band intensity of GAPDH.

A)

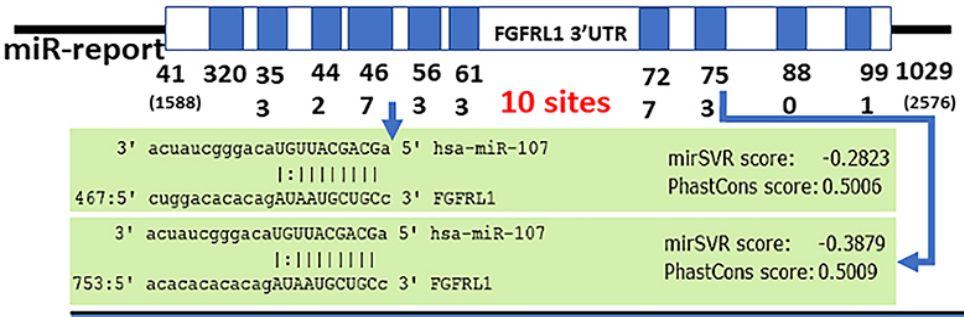

S. No.	Position in mRNA	Position in 3'UTR	Type	miSVR Score
1	1867	320	Canonical 7mer	-0.0788
2	1900	353	Marginal 6mer	-0.0027
3	1989	442	Canonical 7mer	-0.1265
4	2014	467	Canonical 8mer	-0.2823
5	2110	563	Canonical 7mer	-0.1610
6	2160	613	Canonical 7mer	-0.0562
7	2274	727	Canonical 7mer	-0.1881
8	2300	753	Canonical 8mer	-0.3879
9	2427	880	Canonical 7mer	-0.1348
10	2538	991	Canonical 7mer	-0.0574

B)

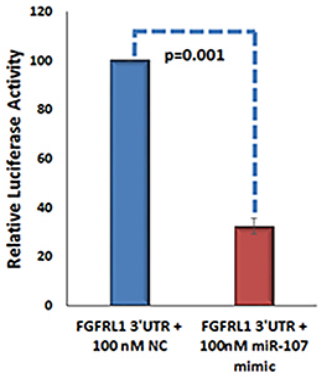

Figure 5. FGFRL1 is a Direct Target of miR-107: A) Figure showing potential binding sites of miR-107 in FGFRL1 3'UTR along with miSVR score and position. miRanda revealed presence of 10 MRE sites for miR-107 in FGFRL1 3'UTR. Canonical 8-mer sites for miR-107 present in FGFRL1 3'UTR are highlighted in red boxes. B) Relative luciferase activity in cells co-transfected with miR-107 mimic and FGFRL1-3′UTR-miR-Report construct in HEK293T cell line as compared to NC at 24 h post transfection; UTR, untranslated region; NC, Negative Control.

of miR-210 which corroborates with our analysis (Eswarakumar et al., 2005; Sharma et al., 2013; Steinberg., 2010). miR-107 had 10 MREs in FGFRL1 3'UTR out of which 9 were canonical 7 or 8 mers suggesting it to be a strong target. Therefore, in order to avoid false positives, we selected miR-107 for further validation using a series of systematic invitro assays.

Correlation between miR-107 and its in-silico predicted target, FGFRL1

miR-107 expression was found to be significantly and inversely correlated with FGFRL1 expression in 72.5% (11/40) esophageal tissues (r=-0.332; p=0.036) suggesting FGFRL1 to be the downstream target of miR-107 (Figure 4B).

Transfection efficiency

Real-time PCR analysis revealed an increase in miR-107 expression by 400-fold at 72 h post miR-107 mimic transfection in the KYSE-410 cells as compared to the cells treated with NC indicating that miR-107 was successfully transfected (Figure 4c).

miR-107 overexpression results in decreased expression of FGFRL1 at the mRNA level

Interestingly, enforced expression of miR-107 in ESCC cell line KYSE-410 significantly decreased expression of FGFRL1 mRNA by 70.05% at 48 h post transfection and 91.69% at 72 h post transfection ($p<0.001$) (Figure 4D). Therefore, we further validated if it is the direct target of miR-107.

Enforced expression of miR-107 results in decreased expression of FGFRL1 protein

To verify that miR-107 acts as a FGFRL1 suppressor, KYSE-410 cells were transfected with 100 nM miR-107 and the NC. The relative expression of FGFRL1 protein was calculated as band intensity of FGFRL1/band intensity of GAPDH. Densitometry analysis showed that at 48 h and 72h post-transfection, overexpression of miR-107 decreased the FGFRL1 protein level by 20% and 57.27% as compared to the NC (Figure 4E).

miR-107 targets FGFRL1-3'UTR directly

To examine whether FGFRL1 is a direct target of miR-107, we looked for the presence of miR-107 target sites in its 3'UTR. Interestingly, miRanda showed presence of ten miR-107 MRE in 3'UTR of FGFRL1 (Figure 5A). It is noteworthy, that out of these ten sites, two were 8-mer canonical sites, 7 were canonical 7-mers and one was marginal site, suggesting it to be a strong target of miR-107. The two 8-mer sites were present at positions 467 and 753 in 3'UTR of FGFRL1 and showed maximum miSVR score of - 0.2823 and -0.3879 respectively. A 989 bp region of FGFRL1-3'UTR (NM_001004358.1) containing all the ten predicted binding sites for miR-107 was cloned in miR-Report vector by our group. Luciferase reporter assay showed that co-transfection of miR-107 and pMIR-FGFRL1- 3'UTR construct in HEK293T cells significantly ($p=0.001$) decreased luciferase activity by 67.62% at 24 h post miR-107 transfection as compared to the NC (Figure 5B).

Discussion

Esophageal Cancer (EC) is the seventh most common cancer in the world (Ferlay et al., 2019). Since its 5 year survival rate is very low, poor outcomes are common even after the symptoms have been accurately correlated (Enzinger et al., 2003; Pennathur et al., 2008) Although treatment options for EC have improved in recent years, the overall prognosis for patients remains very poor (Pennathur et al., 2008). Therefore, in order to identify biomarker and therapeutic targets in EC, investigations into the molecular mechanisms of EC progression are urgent.

FGF/FGFR pathway activation is implicated in the development and progression of a variety of cancers (Jang et al., 2001; Chin et al., 2006; Behrens et al., 2008) FGFRL1 is the fifth and latest addition in the FGFR family of receptor tyrosine kinases. Unlike the other four members of the FGFR family, it lacks the classical kinase domain but has still been shown to activate downstream signal transduction via interaction with key signalling proteins (Gerber et al., 2012; Tai et al., 2018). Although, FGFRL1 has been shown to be aberrantly expressed in SCLC, ovarian cancer (OC), bladder cancer and osteosarcoma, its expression in EC is yet to be investigated (Yang et al., 2017 ; Chen et al., 2020; Liu et al., 2018; Tai st al., 2018). High FGFRL1 levels correlated with poor prognosis in OC and hypoxia induced FGFRL1 expression promoted tumor progression by crosstalk with Hedgehog signalling (Tai et al., 2018). This appears to be consistent with our findings of increased FGFRL1 expression in ESCCs as compared to the distant matched non-malignant tissues.Analysis of data obtained from TCGA and GTeX portals also reveals significant upregulation of FGFRL1 in EC tissues compared to normal controls thus supporting our findings. Deregulation of FGFRs has been attributed to amplification, point mutation, or translocation and amplification being the most common deregulation form in multiple cancer types (Eswarakumar et al., 2005; Helsten et al., 2016 ; Grose et al., 2005). Although FGFR alteration are well studied in several cancers, limited information is available in EC. Recently, Song et al., (2017) investigated the frequency and the prognostic impact of FGFR1 amplification in ESCC patients. They demonstrated that high FGFR1 amplification presented as a delayed adverse prognostic factor in resected stage I-II ESCC patients. FGFRL1 being a relatively new member of the FGFR family has not yet been explored in this regard. cBioPortal showed 6% alterations in the FGFRL1 gene in esophageal tumors and its expression was associated with poor disease-free survival in patients with FGFRL1 alterations as compared to unaltered group, thus further establishing the clinical relevance of FGFRL1 in EC. Moreover, the prevalence of FGFR amplification is the primary determining factor for the efficacy and application of FGFR inhibitors in management of EC patients. This necessitates further well-orchestrated investigation in this area. In regards of potential limitations, our current study is retrospective in nature, and our results must be validated in future prospective studies with follow up samples to validate association of FGFRL1 with prognosis in EC patients.

Aberrant expression of miRNAs contributes significantly to development and progression of cancers by subsequent changes in expression of their target genes. miRNAs regulating FGFRs have been shown to be downregulated in several cancers thereby leading to activation of FGF/FGFR signalling (Wang et al., 2013; Schelch et al., 2018) This is emerging to be another mechanism which might lead to FGFR overexpression in cancers. Herein, using bioinformatics tools viz. mirnet, miRanda, and miRdb, we identified miR-107 to be one of the most potential miRNA that may regulate FGFRL1. Enforced expression of miR-107 in EC cells significantly decreased FGFRL1 mRNA and protein expression and its co-transfection significantly decreased the luciferase activity thus confirming it to be a direct target of miR-107. Moreover, FGFRL1 expression was found to be significantly and negatively correlated with the expression of miR-107 in EC tissues. These results collectively demonstrate miR-107 mediated regulation of FGFRL1 in EC. Our lab has previously reported miR-107 to be a tumor suppressor miRNA. Its overexpression suppressed ESCC cell proliferation and migration and induced G1/S arrest (Sharma et al., 2017; Liu et al., 2018). FGFRL1 has previously been linked with cell proliferation while its downregultion has been shown to cause cell cycle arrest in various cancers (Tsuchiya et al., 2011). Our in-silico analysis identified miR-210 as other potential miRNA targeting FGFRL1. Previous studies corroborate with our finding (Zuo et al., 2015; Huang

et al., 2009). Hypoxia induced miR-210 downregulated the expression of FGFRL1 in laryngocarcinoma thereby promoting cells in G1/G0 phase and decreasing in S and G2/M phases (Zuo et al., 2015). Moreover, FGFRL1 could partially rescue the inhibitory effect of miR-210 on tumor growth in tumor xenografts (Huang et al., 2009). miR-210 directly targeted the 3'UTR site of FGFRL1 and inhibited EC cell proliferation while FGFRL1 accelerated cancer cell proliferation by preventing G0/G1 cell cycle arrest (Tsuchiya et al., 2011). Taken together these studies suggest that FGFRL1 positively regulates cancer cell proliferation including EC and inhibits cell cycle arrest.

In conclusion, using a systematic invitro assays and EC patient samples we established the clinical relevance of FGFRL1 in EC and identified miR-107 mediated regulation as one of the possible mechanisms contributing to its enhanced expression in EC.

Author Contribution Statement

Concept and design: Rinu Sharma; Acquisition, analysis, or interpretation of data: Priyanka Sharma, Vaishali Kaushik, and Rinu Sharma, Drafting of the manuscript: Priyanka Sharma, Vaishali Kaushik, Anoop Saraya and Rinu Sharma; Statistical analysis: Priyanka Sharma, Vaishali Kaushik, and Rinu Sharma; Administrative, technical, or material support: Anoop Saraya and Rinu Sharma; Supervision: Rinu Sharma Priyanka Sharma, Vaishali Kaushik, Anoop Saraya, and Rinu Sharma take responsibility for the integrity of the work.

Acknowledgements

The authors acknowledge and thank CSIR, ICMR, and Guru Gobind Singh Indraprastha University for funding the study.

Funding

This work was supported by FRGS (GGSIPU/DRC/FRGS/2018/19(1115)) and GGSIPU/DRC/FRGS/2021/594/17]., ICMR (2019-0940/GEN/ADHOC/BMS) and CSIR (27(0342)/19/EMR-II).

Ethical Approval

This study was approved by the institutional ethics committee prior to its commencement and informed consent was obtained from each patient. The research was carried out according to the principles set out in the Declaration of Helsinki 1964 and all subsequent revisions.

Reference Number

[GGSIPU/ IEC/ 1.2/2010] ,[IEC/NP-320/2010]

The study was approved by University School Research Committee in addition to Institutional Ethical Committee (GGSIPU and AIIMS , Delhi). This study was a part of an approved thesis of Ph.D. student Dr. Priyanka Sharma.

Data And Materials Availability Statement

Not applicable

Conflict of Interest

The authors have no conflicts of interest to disclose.

References

Behrens C, Lin HY, Lee JJ, et al (2008). Immunohistochemical expression of basic fibroblast growth factor and fibroblast growth factor receptors 1 and 2 in the pathogenesis of lung cancer. *Clin Cancer Res*, **14**, 6014-22.

Bonifacino JS, Traub LM (2003). Signals for sorting of transmembrane proteins to endosomes and lysosomes. *Annu Rev Biochem*, **72**, 395-447.

Carraro G, El-Hashash A, Guidolin D, et al (2009). miR-17 family of microRNAs controls FGF10-mediated embryonic lung epithelial branching morphogenesis through MAPK14 and STAT3 regulation of E-Cadherin distribution. *Dev Biol*, **333**, 238-50.

Chen R, Li D, Zheng M, et al (2020). FGFRL1 affects chemoresistance of small-cell lung cancer by modulating the PI3K/Akt pathway via ENO1. *J Cell Mol Med*, **24**, 2123-34.

Cheng Z, Ma R, Tan W, Zhang L (2014). MiR-152 suppresses the proliferation and invasion of NSCLC cells by inhibiting FGF2. *Exp Mol Med*, **46**, e112.

Chin K, DeVries S, Fridlyand J, et al (2006). Genomic and transcriptional aberrations linked to breast cancer pathophysiologies. *Cancer Cell*, **10**, 529-41.

Di Martino E, Taylor CF, Roulson JA, Knowles MA (2013). An integrated genomic, transcriptional and protein investigation of FGFRL1 as a putative 4p16.3 deletion target in bladder cancer. *Genes Chromosomes Cancer*, **52**, 860-71.

Enzinger PC, Mayer RJ (2003). Esophageal cancer. *N Engl J Med*, **349**, 2241-52.

Eswarakumar VP, Lax I, Schlessinger J (2005). Cellular signaling by fibroblast growth factor receptors. *Cytokine Growth Factor Rev*, **16**, 139-49.

Ferlay J, Colombet M, Soerjomataram I, et al (2019). Estimating the global cancer incidence and mortality in 2018: GLOBOCAN sources and methods. *Int J Cancer*, **144**, 1941-53.

Fu T, Seok S, Choi S, et al (2014). MicroRNA 34a inhibits beige and brown fat formation in obesity in part by suppressing adipocyte fibroblast growth factor 21 signaling and SIRT1 function. *Mol Cell Biol*, **34**, 4130-42.

Gerber SD, Amann R, Wyder S, Trueb B (2012). Comparison of the gene expression profiles from normal and Fgfrl1 deficient mouse kidneys reveals downstream targets of Fgfrl1 signaling. *PLoS One*, **7**, e33457.

Grose R, Dickson C (2005). Fibroblast growth factor signaling in tumorigenesis. *Cytokine Growth Factor Rev*,**16**, 179-86.

Helsten T, Elkin S, Arthur E, et al (2016). The FGFR Landscape in Cancer: Analysis of 4,853 Tumors by Next-Generation Sequencing. *Clin Cancer Res*, **22**, 259-67.

Huang X, Ding L, Bennewith KL, et al (2009). Hypoxia-inducible mir-210 regulates normoxic gene expression involved in tumor initiation. *Mol Cell*, **35**, 856-67.

Jang JH, Shin KH, Park JG (2001). Mutations in fibroblast growth factor receptor 2 and fibroblast growth factor receptor 3 genes associated with human gastric and colorectal cancers. *Cancer Res*, **61**, 3541-3.

Kim J, Kang Y, Kojima Y, et al (2013). An endothelial apelin-FGF link mediated by miR-424 and miR-503 is disrupted in pulmonary arterial hypertension. *Nat Med*, **19**, 74-82.

Liu F, You X, Wang Y, et al (2014). The oncoprotein HBXIP enhances angiogenesis and growth of breast cancer through modulating FGF8 and VEGF. *Carcinogenesis*, **35**, 1144-53.

Liu H, Sun Q, Wan C, et al (2014). MicroRNA-338-3p regulates osteogenic differentiation of mouse bone marrow stromal

stem cells by targeting Runx2 and Fgfr2. *J Cell Physiol*, **229**, 1494-502.
Liu X, Zhang C, Wang C, et al (2018). miR-210 promotes human osteosarcoma cell migration and invasion by targeting FGFRL1. *Oncol Lett*, **16**, 2229-36.
Olsen SK, Ibrahimi OA, Raucci A, et al (2004). Insights into the molecular basis for fibroblast growth factor receptor autoinhibition and ligand-binding promiscuity. *Proc Natl Acad Sci U S A*, **101**, 935-40.
Pennathur A, Luketich JD (2008). Resection for esophageal cancer: strategies for optimal management. *Ann Thorac Surg*, **85**, 751-6.
Rieckmann T, Zhuang L, Fluck CE, Trueb B (2009). Characterization of the first FGFRL1 mutation identified in a craniosynostosis patient. *Biochim Biophys Acta*, **1792**, 112-21.
Schelch K, Kirschner MB, Williams M, et al (2018). A link between the fibroblast growth factor axis and the miR-16 family reveals potential new treatment combinations in mesothelioma. *Mol Oncol*, **12**, 58-73.
Sharma P, Saini N, Sharma R (2017). miR-107 functions as a tumor suppressor in human esophageal squamous cell carcinoma and targets Cdc42. *Oncol Rep*, **37**, 3116-27.
Sharma P, Saraya A, Gupta P, Sharma R (2013). Decreased levels of circulating and tissue miR-107 in human esophageal cancer. *Biomarkers*, **18**, 322-30.
Silva PN, Altamentova SM, Kilkenny DM, Rocheleau JV (2013). Fibroblast growth factor receptor like-1 (FGFRL1) interacts with SHP-1 phosphatase at insulin secretory granules and induces beta-cell ERK1/2 protein activation. *J Biol Chem*, **288**, 17859-70.
Song Q, Liu Y, Jiang D, et al (2017). High amplification of FGFR1 gene is a delayed poor prognostic factor in early stage ESCC patients. *Oncotarget*, **8**, 74539-53.
Steinberg F, Gerber SD, Rieckmann T, Trueb B (2010). Rapid fusion and syncytium formation of heterologous cells upon expression of the FGFRL1 receptor. *J Biol Chem*, **285**, 37704-15.
Steinberg F, Zhuang L, Beyeler M, et al (2010). The FGFRL1 receptor is shed from cell membranes, binds fibroblast growth factors (FGFs), and antagonizes FGF signaling in Xenopus embryos. *J Biol Chem*, **285**, 2193-202.
Stephens P, Edkins S, Davies H, et al (2005). A screen of the complete protein kinase gene family identifies diverse patterns of somatic mutations in human breast cancer. *Nat Genet*, **37**, 590-2.
Tai H, Wu Z, Sun S, Zhang Z, Xu C (2018). FGFRL1 Promotes Ovarian Cancer Progression by Crosstalk with Hedgehog Signaling. *J Immunol Res*, **2018**, 7438608.
Tang Z, Li C, Kang B, et al (2017). GEPIA: a web server for cancer and normal gene expression profiling and interactive analyses. *Nucleic Acids Res*, **45**, 98-102.
Trueb B, Zhuang L, Taeschler S, Wiedemann M (2003). Characterization of FGFRL1, a novel fibroblast growth factor (FGF) receptor preferentially expressed in skeletal tissues. *J Biol Chem*, **278**, 33857-65.
Tsuchiya S, Fujiwara T, Sato F, et al (2011). MicroRNA-210 regulates cancer cell proliferation through targeting fibroblast growth factor receptor-like 1 (FGFRL1). *J Biol Chem*, **286**, 420-8.
Turner N, Grose R (2010). Fibroblast growth factor signalling: from development to cancer. *Nat Rev Cancer*, **10**, 116-29.
Uchiyama K, Naito Y, Takagi T, et al (2010). Carbon monoxide enhance colonic epithelial restitution via FGF15 derived from colonic myofibroblasts. *Biochem Biophys Res Commun*, **391**, 1122-6.
Wang J, Li J, Wang X, Zheng C, Ma W (2013). Downregulation of microRNA-214 and overexpression of FGFR-1 contribute to hepatocellular carcinoma metastasis. *Biochem Biophys Res Commun*, **439**, 47-53.
Wang L, He J, Hu H, et al (2020). Lung CSC-derived exosomal miR-210-3p contributes to a pro-metastatic phenotype in lung cancer by targeting FGFRL1. *J Cell Mol Med*, **24**, 6324-39.
Wesche J, Haglund K, Haugsten EM (2011). Fibroblast growth factors and their receptors in cancer. *Biochem J*, **437**, 199-213.
Wiedemann M, Trueb B (2000). Characterization of a novel protein (FGFRL1) from human cartilage related to FGF receptors. *Genomics*, **69**, 275-9.
Yang J, Zhao H, Xin Y, Fan L (2014). MicroRNA-198 inhibits proliferation and induces apoptosis of lung cancer cells via targeting FGFR1. *J Cell Biochem*, **115**, 987-95.
Yang X, Shi L, Yi C, et al (2017). MiR-210-3p inhibits the tumor growth and metastasis of bladder cancer via targeting fibroblast growth factor receptor-like 1. *Am J Cancer Res*, **7**, 1738-53.
Yang Y, Zhang J, Xia T, et al (2016). MicroRNA-210 promotes cancer angiogenesis by targeting fibroblast growth factor receptor-like 1 in hepatocellular carcinoma. *Oncol Rep*, **36**, 2553-62.
Yin Y, Betsuyaku T, Garbow JR, et al (2013). Rapid induction of lung adenocarcinoma by fibroblast growth factor 9 signaling through FGF receptor 3. *Cancer Res*, **73**, 5730-41.
Zhuang L, Villiger P, Trueb B (2011). Interaction of the receptor FGFRL1 with the negative regulator Spred1. *Cell Signal*, **23**, 1496-504.
Zuo J, Wen M, Lei M, et al (2015). MiR-210 links hypoxia with cell proliferation regulation in human Laryngocarcinoma cancer. *J Cell Biochem*, **116**, 1039-49.